Step and Pulse Response Methods for Identification of Wiener Processes

Ho Cheol Park and Jietae Lee
Dept. of Chemical Engineering, Kyungpook National University, Daegu 702–701, Korea

DOI 10.1002/aic.10690
Published online October 4, 2005 in Wiley InterScience (www.interscience.wiley.com).

Lack of simple identification methods for nonlinear processes hinders field applications of nonlinear control systems. For identification methods that are as simple as those for the first order plus time delay models of linear dynamical processes, graphical and least squares methods to identify Wiener-type nonlinear processes from standard responses, such as step, pulse, and square-wave responses, are proposed. Static nonlinear functions are identified independently in Wiener-type nonlinear processes. Graphical methods extract discrete points of the nonlinear static function or a continuous non-parametric model of the nonlinear static function iteratively. The least squares method provides a parametric model of the nonlinear static function. The identified static nonlinear function can be used to design a simple linearizing control system. To illustrate the proposed identification methods, simulation and experimental results are given. *AIChE J,* 52: 668–677, 2006
Keywords: Wiener-type nonlinear process, identification, step response, pulse response, relay feedback

Introduction

Linear models can approximate the dynamics of industrial chemical processes in limited operating regions. When extended operating regions are required due to large disturbances or set point changes, the nonlinearities in processes cannot be neglected. For this, nonlinear block oriented models that consist of linear dynamic subsystems and memory-less nonlinear static functions, such as Wiener, Hammerstein, and Hammerstein-Wiener models,[1] can be used. Some processes, such as pH processes, can be described by nonlinear block oriented models, and some processes can be approximated well by these block oriented models.

Much effort has been made in estimating the block oriented nonlinear models empirically with approximating static nonlinear functions by cubic spline functions,[2] polynomials,[3] and piecewise linear functions.[4] Pottmann et al.[5] suggested an identification method based on a multi-model approach with Kolmogorov-Gabor polynomials. Bai[6] proposed an optimal two-stage identification algorithm for the Hammerstein-Wiener systems. Sung[7] used random binary signals to identify the linear dynamic subsystem while deactivating effects of the nonlinear elements of the Hammerstein processes. Several authors[8-10] identified the Hammerstein processes by using relay feedback experiments. Applications of nonlinear block oriented models to chemical processes were summarized in Henson and Seborg.[11]

To estimate the Wiener-type nonlinear processes where nonlinear static functions follow linear dynamic subsystems, Luyben and Eskinat[10] used two autotune tests with different relay heights and different dynamic elements inserted in the feedback loop. More elaborate analyses of two relay feedback tests have been made by several authors.[12] Huang et al.[13] suggested a method to classify and identify nonlinear processes using two relay feedback tests. They obtained a few points of the nonlinear function. Sung and Lee[14] proposed a method to identify the nonlinear static function by using one relay feedback test under the assumption that the output of a linear dynamic subsystem is near sinusoidal. Kalafatis et al.[3] used sinusoidal signals to identify the Wiener-type nonlinear process. Their

Correspondence concerning this article should be addressed to J. Lee at jtlee@knu.ac.kr.

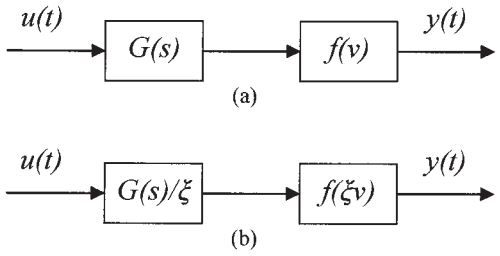

Figure 1. Two equivalent Wiener-type nonlinear processes.

approaches can obtain models described by the frequency response for the linear subsystem and the inverse of the static nonlinearity. Bai[15] proposed a frequency domain identification algorithm of the Wiener-type nonlinear process based on frequency components contained in the process output.

In the present study, graphical and least squares methods to identify the Wiener-type nonlinear processes are proposed. Standard responses, such as two step responses with different sizes, step, and pulse responses or two square-wave responses, are used. The identification of the nonlinear static function is independent of that of the linear dynamic subsystem, simplifying the problem significantly. The graphical methods visualize the identification procedures and are easily understandable. They are as simple as those finding first order plus time delay models for linear dynamic processes. The estimated models can be used to design simple linearizing control systems where nonlinearities of Wiener-type nonlinear processes are removed in the feedback loop. The advantages of proposed identification procedures are demonstrated with simulations and an experiment.

Wiener Process Identification

A Wiener-type nonlinear process in which a linear dynamic subsystem is followed by a static nonlinear function as shown in Figure 1a is considered. It can be represented by

$$V(s) = G(s)U(s) \tag{1}$$

$$y(t) = f(v(t)) \tag{2}$$

where $u(t)$, $v(t)$, and $y(t)$ denote the process input, the intermediate variable of the dynamical subsystem output, and the process output, respectively. It is assumed that the linear dynamic subsystem is stable and that the nonlinear static function $f(v)$ is continuous and strictly monotone with $f(0) = 0$.

The intermediate variable $v(t)$ is not measured and can be scaled as shown in Figure 1b without loss of generality; i.e., the size of $v(t)$ can be arbitrarily assumed. For example, we can set the maximum of $v(t)$ to be 1, $G(0) = 1$ or $f'(0) = 1$. This property is utilized to derive our identification methods.

Step Responses Method—Graphical 1 (ST-G1)

Two step inputs with magnitudes of 1 and α ($0 < \alpha < 1$) are considered, as shown in Figure 2. Let the step inputs be $u_1(t)$ and $u_a(t)$, the intermediate variables be $v_1(t)$ and $v_\alpha(t)$, and the output variables be $y_1(t)$ and $y_\alpha(t)$ for step changes of 1 and α, respectively. Since the intermediate variable $v(t)$ is the output of the linear dynamic subsystem, we have

$$v_\alpha(t) = \alpha v_1(t) \tag{3}$$

Since the intermediate variable $v(t)$ can be arbitrarily scaled, the maximum of $v_1(t)$ is set as 1. Under this assumption, the maximum of $y_1(t)$ is $f(1)$. The maximum of $v_a(t)$ is a (Eq. 3) because that of $v_1(t)$ is 1, and hence the maximum of $y_a(t)$ is $f(a)$. Because the nonlinear function $f(v)$ is assumed to be strictly monotone, $v_1(t_{a1}) = a$ and $v_a(t_{a1}) = av_1(t_{a1}) = a^2$ at the time t_{a1} such that $y_1(t_{a1}) = f(a)$. Hence, $y_a(t_{a1})$ is $f(a^2)$. In this manner, as shown in Figure 2, we can find $f(a^i)$ as

$$f(\alpha^i) = y_\alpha(t_{\alpha i}), \quad i = 1, 2, \ldots \tag{4}$$

where t_{ai} is such that $y_1(t_{ai}) = y_a(t_{a(i-1)}) = f(a^{i-1})$. Some discrete points of $f(v)$ are obtained.

It should be noted that the test input should be large enough so that $y_1(t)$ covers the required region of $f(v)$. The size of the smaller test input should be carefully chosen. When α is chosen to be near 1, $y_1(t)$ and $y_\alpha(t)$ will be close and the identification results can be deteriorated by measurement errors. On the other hand, when α is chosen to be too small, function values near $f(1)$ can be coarse.

The parametric function of $f(v)$ can be obtained by interpolating discrete points of $f(v)$. Since $v(t)$ is also obtained, the linear dynamic subsystem can be identified by applying identification methods for linear dynamical processes.[16]

This method can be used for general linear dynamical subsystems whenever they are stable. Figure 3 shows the identi-

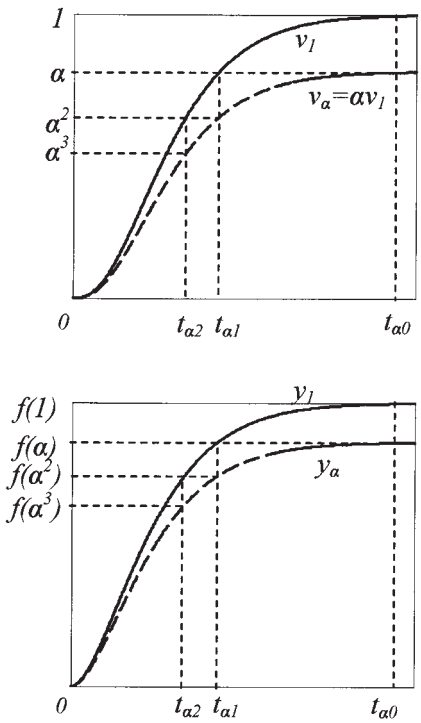

Figure 2. Two step responses with different sizes and the identification procedure for ST-G1 method.

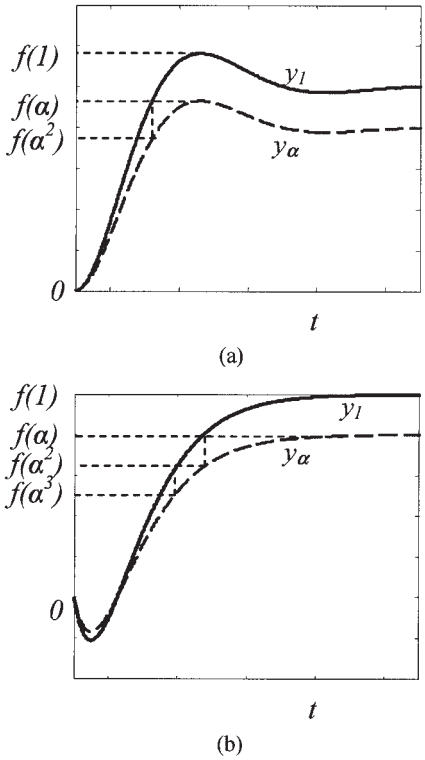

Figure 3. The identification procedures of ST-G1 for underdamped linear subsystem (a) and linear subsystem with inverse response (b).

fication procedures for an underdamped linear subsystem and a linear subsystem with an inverse response. For an underdamped linear subsystem, the response between 0 and the first peak is used for identification. The first peak value of $v_1(t)$ is set to 1. Hence, the peak value of $y_1(t)$ is $f(1)$. Other points of $f(v)$ are shown in Figure 3a. For a linear subsystem with inverse response, the identification procedure is identical to that of the above overdamped subsystem. However, it does not cover the inverse response region. That part should be extrapolated.

Step Responses Method—Graphical 2 (ST-G2)

The above ST-G1 method finds function values at discrete points. A method to obtain continuous non-parametric functions of $f(v)$ is derived here.

When the step size α is small, the intermediate variable $v_\alpha(t)$ will be small and linear approximation of $y_a(t) = f(v_\alpha(t)) \approx v_\alpha(t)$ will be effective. Thus, we have

$$v_1(t) = v_\alpha(t)/\alpha \approx y_\alpha(t)/\alpha \tag{5}$$

The nonlinear static function can be estimated from $y_1(t) = f(v_1(t))$ by mapping $y_1(t)$ and $v_1(t) \approx y_\alpha(t)/\alpha$.

When a is large, the above approximation may not be tolerable. Errors in approximating $v_1(t)$ by Eq. 5) can be eliminated by iteration.

Step 1) Let $v_1^0(t) = y_\alpha(t)/\alpha$.

Step 2) For $k = 1,2,\ldots$, calculate the following until $v_1^k(t)$ converges:

$f_k(\bullet)$: mapping between $y_1(t)$ and $v_1^{k-1}(t)$ (i.e., $y_1(t) = f_k(v_1^{k-1}(t))$) (6)

$$v_1^k(t) = f_k^{-1}(y_\alpha(t))/\alpha \tag{7}$$

In Step 2, $f_k(\bullet)$ is given in a graphical form (or a tabular form), and its inverse can be read with changing the roles of the axes. When $f'(0)$ is neither zero nor infinity, the above iteration converges. Convergence proof is given in the Appendix. When $f'(0)$ is equal to zero or infinity, different operating points should be chosen.

Step Responses Method—Least Squares (ST-LS)

A method to find a parametric model of the nonlinear static function is derived here. Since $y_a(t) = f(v_a(t)) = f(av_1(t))$ and $y_1(t) = f(v_1(t))$, we have

$$f^{-1}(y_1(t)) = f^{-1}(y_\alpha(t))/\alpha \tag{8}$$

From this relationship, a parametric model of the nonlinear static function can be estimated.

For example, let

$$f^{-1}(y) = y + c_2y^2 + c_3y^3 + \cdots + c_ny^n \tag{9}$$

under the assumption that $f(0) = 0$ and $f'(0) = 1$. Then Eq. 8 becomes $y_1(t) + c_2y_1^2(t) + \cdots + c_ny_1^n(t) = (y_\alpha(t) + c_2y_\alpha^2(t) + \cdots + c_ny_\alpha^n(t)/\alpha$
and we have

$$\eta_{ST}(t)\theta = -y_1(t) + y_\alpha(t)/\alpha \tag{10}$$

where $\eta_{ST}(t) = [y_1^2(t) - y_\alpha^2(t)/\alpha, y_1^3(t) - y_\alpha^3(t)/\alpha, \cdots, y_1^n(t) - y_\alpha^n(t)/\alpha]$ and $\theta = [c_2, c_3, \cdots, c_n]^T$. Applying the least squares method, we can obtain the parameter vector θ:

$$\theta = (X^TX)^{-1}X^TY \tag{11}$$

where

$$X = \begin{bmatrix} \eta_{ST}(t_1) \\ \eta_{ST}(t_2) \\ \vdots \\ \eta_{ST}(t_m) \end{bmatrix}, \quad Y = \begin{bmatrix} -y_1(t_1) + y_\alpha(t_1)/\alpha \\ -y_1(t_2) + y_\alpha(t_2)/\alpha \\ \vdots \\ -y_1(t_m) + y_\alpha(t_m)/\alpha \end{bmatrix}$$

Time points, t_i's, are chosen to be equally spaced ($m > n - 1$) and span the whole transient region. The optimal number of terms in Eq. 9 will differ from problem to problem. Some trials in choosing n may be required.

This method can also be applied for noisy responses, and effects of noise including other properties of the least squares method can be found in Ljung.[16] For some nonlinear static functions, polynomial expressions are not adequate and other function forms that are linear in coefficients, such as spline functions, piece-wise linear functions, and artificial neural nets,[17] should be used.

For other inputs such that $u_a(t) = au_1(t)$, $v_a(t) = av_1(t)$ and Eq. 8 are still valid. This least squares method can be applied to such inputs. They are useful for identifying a complicated

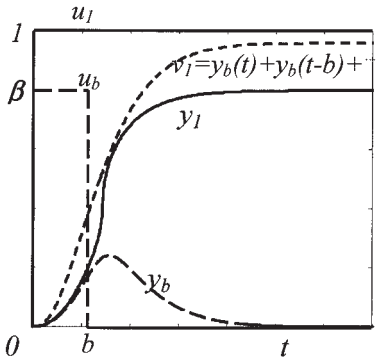

Figure 4. Step and pulse response method.

linear dynamical subsystem from the input $u(t)$ and the intermediate variable estimated by $v(t) = f^{-1}(y(t))$.

Step and Pulse Response Methods (SP)

Instead of a step input with a small magnitude, a pulse input with a small duration can be used. Let $v_b(t)$ and $y_b(t)$ be the intermediate variable and the output variable for a pulse input $u_b(t)$ whose size is β and duration is b (Figure 4), respectively. For step and pulse responses, identification methods similar to the ST-G2 and ST-LS methods can be obtained.

Since $v_1(t)$ and $v_b(t)$ are outputs of the linear subsystem, the superposition rule of the linear system gives

$$v_1(t) = (v_b(t) + v_b(t - b) + v_b(t - 2b) + \cdots + v_b(t - Mb))/\beta \quad (12)$$

for t less than t_m, where M is the largest integer to t_m/b, and t_m is the time span of transient region of $y_1(t)$. Assuming that $v_b(t)$ is sufficiently small so that $f(v) \approx v$ is effective, we have $v_b(t) \approx y_b(t)$ and

$$v_1(t) \approx \frac{1}{\beta} \sum_{k=0}^{M} y_b(t - kb) \quad (13)$$

The nonlinear static function can be estimated from $y_1(t) = f(v_1(t))$ by mapping $y_1(t)$ and $v_1(t)$ of Eq. 13. Figure 4 shows this procedure. Errors in Eq. 13 can also be reduced by iteration. We call this method SP-G2.

Since $y_b(t) = f(v_b(t))$ and $y_1(t) = f(v_1) = f((1/\beta) \sum_{k=0}^{M} v_b(t - kb))$, we have

$$\beta f^{-1}(y_1(t)) = \sum_{k=0}^{M} f^{-1}(y_b(t - kb)) \quad (14)$$

For the polynomial model of Eq. 9, we have

$$\eta_{SP}(t)\theta = -\beta y_1(t) + \sum_{k=0}^{M} y_b(t - kb)$$

$$\eta_{SP}(t) = \begin{bmatrix} \beta y_1^2(t) - \sum_{k=0}^{M} y_b^2(t - kb) \\ \beta y_1^3(t) - \sum_{k=0}^{M} y_b^3(t - kb) \\ \vdots \\ \beta y_1^n(t) - \sum_{k=0}^{M} y_b^n(t - kb) \end{bmatrix}^T, \quad \theta = [c_2, c_3, , c_n]^T \quad (15)$$

Applying the least squares method to Eq. 15, the parameter vector q can be obtained as

$$\theta = (X^T X)^{-1} X^T Y$$

$$X = \begin{bmatrix} \eta_{SP}(t_1) \\ \eta_{SP}(t_2) \\ \vdots \\ \eta_{SP}(t_m) \end{bmatrix}, \quad Y = \begin{bmatrix} -\beta y_1(t_1) + \sum_{k=0}^{M} y_b(t_1 - kb) \\ -\beta y_1(t_2) + \sum_{k=0}^{M} y_b(t_2 - kb) \\ \vdots \\ -\beta y_1(t_m) + \sum_{k=0}^{M} y_b(t_m - kb) \end{bmatrix} \quad (16)$$

We call this method SP-LS. It should be noted that we can choose $b = 1$ and, in this case, the input $u(t)$ has binary values of 0 and 1 and a relay-type actuator can be used.

Square Wave Response Methods (SQ)

Two square wave inputs with magnitudes of 1 and α can be used for simple identification of the Wiener-type nonlinear process. Typical responses of $y_1(t)$ and $y_\alpha(t)$ for square wave inputs with magnitudes of 1 and a are shown in Figure 5. We have $v_\alpha(t) = \alpha v_1(t)$ as in the step response case. Assuming an appropriate scaling, we can set the maximum of $v_1(t)$ to be 1. Hence, the maximum value of $y_1(t)$ is $f(1)$ and the maximum value of $y_\alpha(t)$ is $f(\alpha)$. Values of $f(v)$ at the corresponding points of $\{1, \alpha, \alpha^2, \ldots\}$ are easily obtained, as shown in Figure 5. This procedure can be applied to the positive rising, positive falling, negative rising, and negative falling parts of responses. These square wave responses can be obtained by relay feedback with different relay magnitudes.

For square-wave responses of $y_1(t)$ and $y_\alpha(t)$, Eqs. 3 and 8 are also valid. Hence, methods used for ST-G2 and ST-LS can be applied for the square wave responses. We call the square wave response methods corresponding to the ST-G1, ST-G2, and ST-LS methods by SQ-G1, SQ-G2, and SQ-LS, respectively.

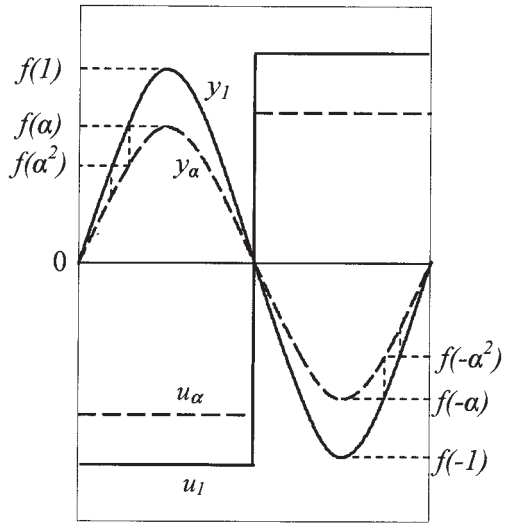

Figure 5. Square wave response method.

Linearizing Control Systems

Once the static nonlinear function in the Wiener-type nonlinear process is obtained, a simple linearizing control system[14] can be designed. As shown in Figure 6, the inverse of a nonlinear static function linearizes the Wiener-type nonlinear process. Because the nonlinear part is removed in the feedback loop, the linear controller $G_c(s)$ can be designed for the linear dynamic subsystem. Various tuning rules, such as the ZN tuning method and the optimal tuning method,[18,19] can be applied for PI/PID control of the linearized process.

The control system in Figure 6 does not linearize the input-output behavior between the set point and the output and, furthermore, the feedback loop also cannot be linear when estimated nonlinear functions have errors. Detailed robustness analyses might be needed, but they are beyond the scope of this article. Instead, we illustrate through simulations and experimental examples that the linearizing control system works well despite estimation errors in the nonlinear static function.

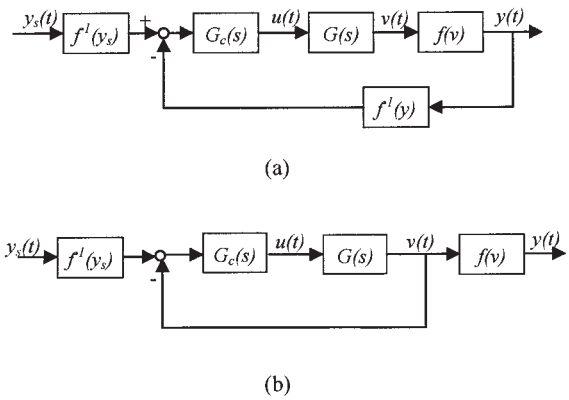

Figure 6. Linearizing control system (a) and equivalent control system (b).

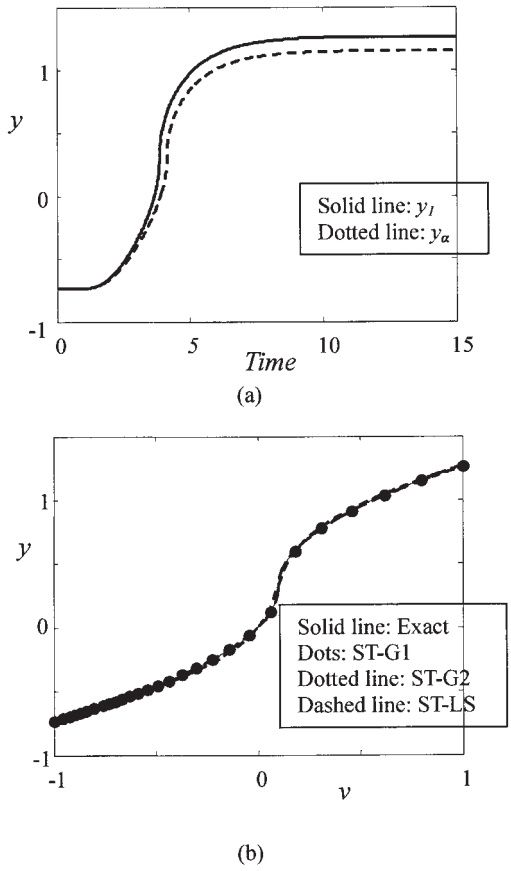

Figure 7. Step response methods for Example 1.

(a) Two step responses, and (b) identification results for the nonlinear static function.

Simulation Examples

Example 1

Consider the following Wiener-type nonlinear process in which the linear dynamic subsystem is a third order plus time delay model and the nonlinear static function is a square root function.

$$V(s) = G(s)U(s) = \frac{\exp(-s)}{(s+1)^3}\,U(s) \tag{17}$$

$$y(t) = \begin{cases} -\sqrt{|v(t) - 0.1|} + \sqrt{0.1} & \text{for } v(t) < 0.1 \\ \sqrt{v(t) - 0.1} + \sqrt{0.1} & \text{for } v(t) \geq 0.1 \end{cases} \tag{18}$$

The process is first at the steady state of $u_{ss} = -1$ and $y_{ss} = \sqrt{0.1} - \sqrt{1.1}$ and is activated by two step inputs with magnitudes of 2 and 1.8. New deviation variables of $\tilde{v}(t) = v(t) + 1$ and $\tilde{y}(t) = y(t) - (\sqrt{0.1} - \sqrt{1.1})$ are defined, and their nonlinear relationship

$$\tilde{y}(t) = \begin{cases} -\sqrt{|\tilde{v}(t) - 1.1|} + \sqrt{1.1} & \text{for } \tilde{v}(t) < 1.1 \\ \sqrt{\tilde{v}(t) - 1.1} + \sqrt{1.1} & \text{for } \tilde{v}(t) \geq 1.1 \end{cases} \tag{19}$$

is identified. Step responses are shown in Figure 7a, and three identification methods (ST-G1, ST-G2, and ST-LS) are ap-

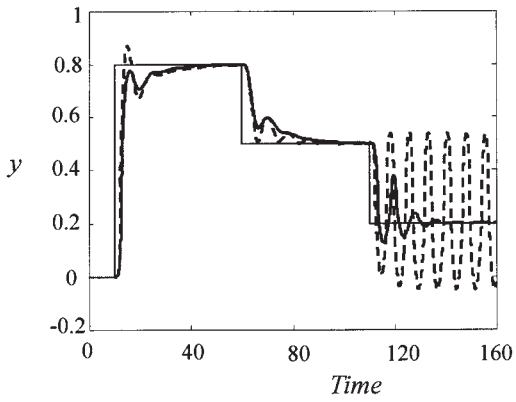

Figure 8. Control results for Example 1 (thin solid line: set point, dotted line: conventional PI controller, thick solid line: linearizing PI controller).

plied. Results in the deviation variables of $\tilde{v}(t)$ and $\tilde{y}(t)$ are rewritten by the original variables of $v(t)$ and $y(t)$.

Figure 7b shows identification results. Because each identification method has a different scaling, we adjusted the size of the estimated nonlinear function for comparison. However, to design a linearizing control system, it is unnecessary to adjust the scale of the nonlinear static function. We can see that estimated nonlinear functions show excellent agreement with the real nonlinear function. The ST-LS method provides an inverse parametric model of the nonlinear function as

$$v(t) = y(t) - 1.84y^2(t) + 1.68y^3(t) + 0.86y^4(t) - 0.61y^5(t) \tag{20}$$

Step and pulse response methods and square wave response methods are also tested. Very similar results are obtained.[20] A parametric model obtained by the SP-LS method is

$$v(t) = y(t) - 1.65y^2(t) + 1.48y^3(t) + 0.82y^4(t) - 0.58y^5(t) \tag{21}$$

We can see that both polynomial functions of Eqs. 20 and 21 are very close to the real nonlinear static function.

A linear dynamic model is required to design the linear controller $G_c(s)$ in Figure 6a. From the unit step input $u_1(t)$ and $v_1(t)$ estimated by the ST-LS method, we obtained the following first order plus time delay model by the area method based on the step response.[18]

$$\frac{V(s)}{U(s)} = \frac{1.8513\ \exp(-2.2015s)}{1.77966s + 1} \tag{22}$$

Figure 8 shows the control performances of the conventional PI controller and the linearizing PI controller tuned by the ZN tuning rule.[19] Eq. 20 is used as the inverse of the nonlinear function. The linearizing controller shows good control performances for the set point changes because it compensates the nonlinear dynamics regardless of the set point values. However, the conventional PI controller shows oscillatory responses for some set point values.

The proposed methods can also be applied to other Wiener-type nonlinear processes, such as those with dead zone nonlinearities under noisy environments. Identification results for such processes are given in Park.[20]

Example 2

For a practical application, we consider a pH neutralization process, which is important in various chemical processes such as wastewater treatment processes, biochemical processes, and polymerization processes. Because of strong nonlinearities, it is difficult to control the pH neutralization processes.

A simple schematic diagram is shown in Figure 9, where the influent stream of the acetic acid (CH_3COOH) is titrated by the strong base of sodium hydroxide (NaOH) in a continuous stirred tank reactor. It is assumed that the volume of the reactor is constant and that the acid-base reaction is very fast. The mathematical model equations are given as follows.[21,22]

$$V\frac{dc_a(t)}{dt} = -(F + u(t))c_a(t) + Fc_{f,a}$$

$$V\frac{dc_b(t)}{dt} = -(F + u(t))c_b(t) + u(t)c_{c,b} \tag{23}$$

$$-\frac{K_a c_a(t)}{K_a + z(t)} + c_b(t) + z(t) - \frac{K_w}{z(t)} = 0$$

$$\mathrm{pH} = -\log_{10}(z(t)) \tag{24}$$

Variables are explained in Table 1.

Wright and Kravaris[21] have shown that, with introducing an intermediate variable c_b (named a total ion concentration), the model equations of Eqs. 23 and 24 can be reduced to the following equations:

$$V\frac{dc_b(t)}{dt} = -(F + u(t))c_b(t) + u(t)c_{c,b} \tag{25}$$

$$-\frac{K_a c_{f,a}}{K_a + z(t)} + c_b(t) + z(t) - \frac{K_w}{z(t)} = 0$$

$$\mathrm{pH} = -\log_{10}(z(t)) \tag{26}$$

Because a concentrated titrating base is usually used, the flow rate of the titrating stream is very small ($u(t) \ll F$) and the dynamic equations of Eq. 25 are almost linear. The nonlinearity of the pH neutralization process is mainly due to the titration curve equation of Eq. 26. This pH neutralization process can be regarded as a Wiener-type nonlinear process in which the nonlinear function is the titration curve.

The proposed identification methods are applied to estimate the titration curve. The simulation data are shown in Table 1. The pH process is activated by step and pulse inputs and relay feedback. An artificial time delay of 1 minute is inserted into the relay feedback loop for a stable oscillation with a proper period. The activated process outputs are shown in Figure 10. Estimated titration curves are compared with the real titration curve in Figure 11. Since each identification method provides a titration curve model in a deviation variable and has a

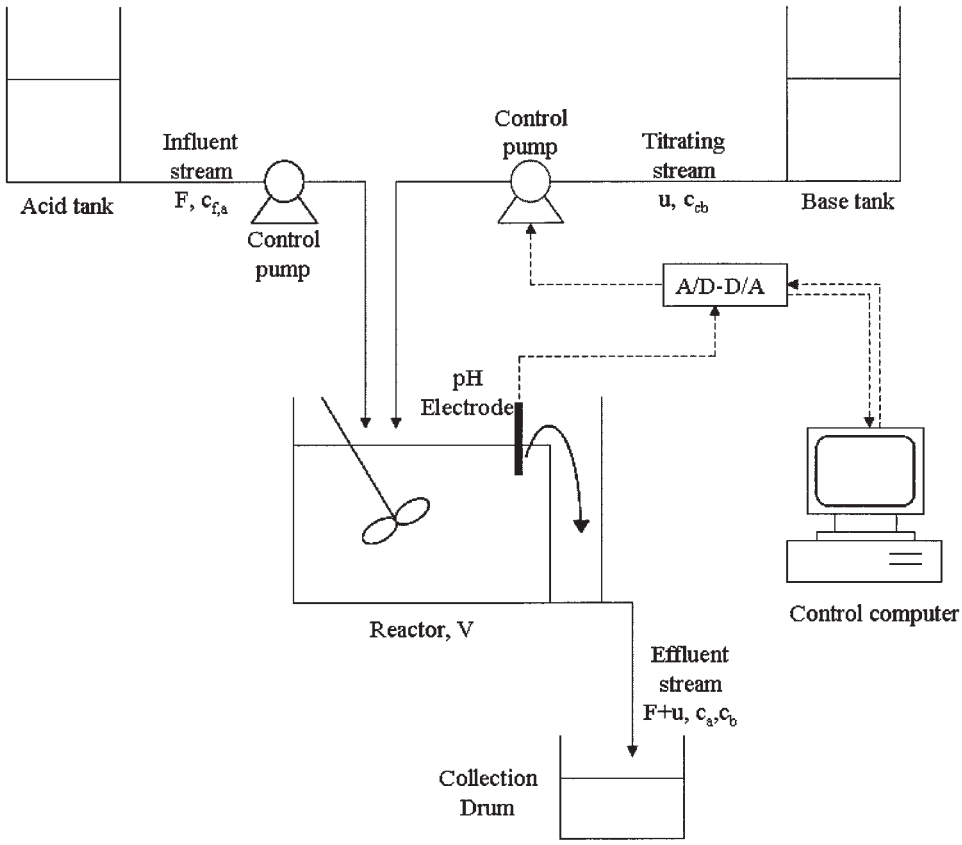

Figure 9. pH neutralization process.

different scaling, we adjust the identified models so that the intermediate variable of the estimated model is the same as the scaled total ion concentration, $c_b/c_{c,b}$, of the real titration curve. Fifth order polynomials for the estimated inverse model of the titration curves are given in Park.[20] Among them, a model obtained by the ST-LS method is:

$$\frac{c_b(t)}{c_{c,b}} = -1.1495 + 0.70901\,\mathrm{pH}(t) - 0.16874\,\mathrm{pH}^2(t) + 2.0014 \times 10^{-2}\,\mathrm{pH}^3(t) - 1.1826 \times 10^{-3}\,\mathrm{pH}^4(t) + 2.7854 \times 10^{-5}\,\mathrm{pH}^5(t) \quad (27)$$

We can see that the estimated titration curves describe the real titration curve well.

Table 1. Simulation Data for the pH Neutralization Process

K_w: dissociation constant of water = 1.0×10^{-14}
K_a: dissociation constant of CH_3COOH = 1.8×10^{-5}
$c_{f,a}$: total ion concentration of the acetic acid in the influent stream = 0.02 mol/L
$c_{c,b}$: total ion concentration of the sodium hydroxide in the titrating stream = 0.5 mol/L
c_a: total ion concentration of the acetic acid in the effluent stream: 0.0193 mol/L at $t = 0$
c_b: total ion concentration of the sodium hydroxide in the effluent stream: 0.0183 mol/L at $t = 0$
F: flow rate of influent stream = 1 L/min
$u(t)$: flow rate of the titrating stream
V: reactor volume = 5 L
$z(t)$: hydrogen ion concentration
Sampling time: 0.1 min

Step and pulse inputs:
Initial flow rate of titrating stream = 0.0379 L/min
Magnitudes of step inputs = 0.0042 L/min and 0.0038 L/min
Magnitude of pulse input = 0.0038 L/min
Width of pulse input = 1 min

Relay feedback system:
Set point of relays = 7
Flow rate of titrating stream corresponding to set point = 0.0398 L/min
Magnitudes of relays = 0.0038 L/min and 0.0030 L/min

Experimental Example

The pH neutralization process simulated in Example 2 was experimentally tested. The equipment consisted of an acid tank (80L), a base tank (20L), two control pumps, a reactor (2.67L), a pH sensor, an A/D-D/A converter, and a control computer. The control pump at the influent stream was set to maintain approximately a constant flow rate of 0.4L/min. The flow rate of the control pump at the titrating stream was determined by the control computer and transmitted to the control pump through the A/D-D/A converter. Although the relationship between the signal sent to the pump and the resulting flow rate was slightly nonlinear, we regarded it as linear. Slight fluctuations appeared in the flow rates due to the characteristics of pumps. Both the influent stream and the titrating stream entered the reactor simultaneously and were mixed by the stirrer. To prevent bypass flow, the influent stream and the titrating stream

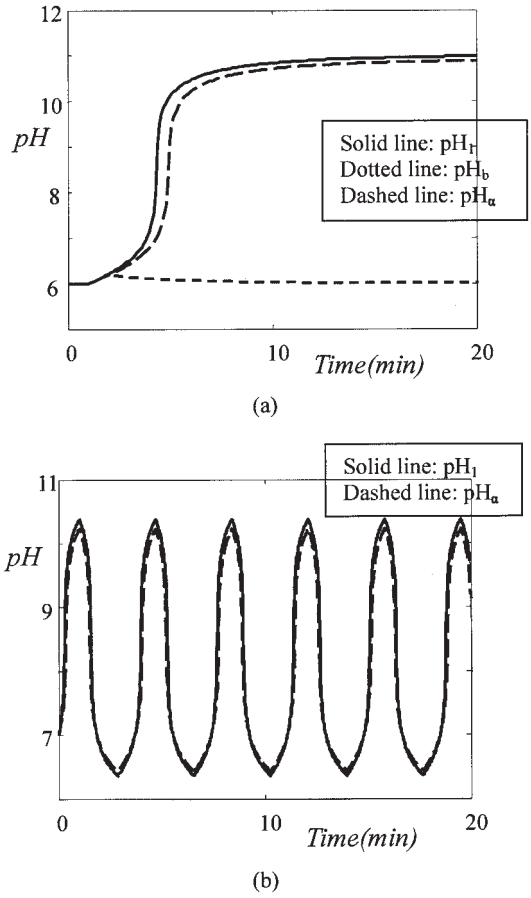

Figure 10. Responses of the simulated pH neutralization process for step and pulse inputs (a) and relay feedback systems (b).

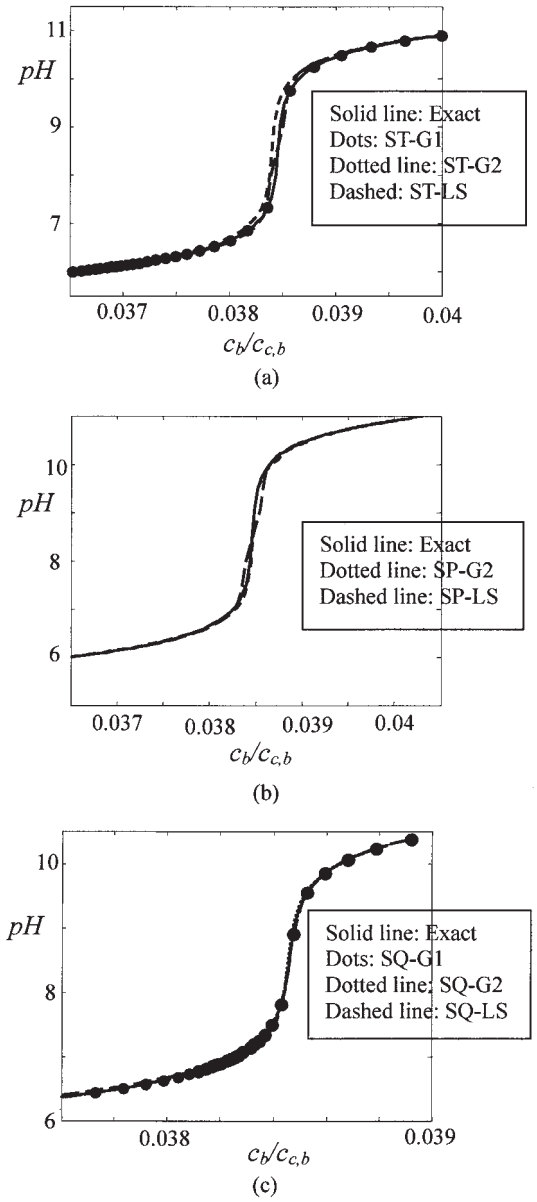

Figure 11. Estimated titration curves for the simulated pH neutralization process.

(a) Step response methods, (b) step and pulse response methods, and (c) square wave response methods.

were injected from the bottom of the reactor. A baffle was used for a constant volume of the reactor without a level control. The effluent stream overflowed from the reactor. The pH sensor was submerged near the exit of the effluent stream in the reactor. The pH measurement signal was transmitted to the control computer through the A/D-D/A converter. The pH sensor dynamics was neglected because it was small compared with the dynamics of the reactor. The control computer received the pH signal from the pH sensor through the A/D-D/A converter and sent the flow rate signal to the control pump in the titrating stream. A lab-made A/D-D/A converter with a low noise 16-bit resolution for A/D and a 14-bit resolution for D/A was used. The detailed experimental data are shown in Table 2.

Step inputs and the pulse input in Table 2 are used to activate the pH neutralization process. Figure 12 shows the activated process outputs. The titration curve is identified from activated process outputs using the proposed methods. The identified titration curve models are adjusted as in the simulation Example 2. Figure 13 shows the estimated titration curves and the real titration curve. The real titration curve is obtained by titrating the influent stream with standard solutions. We can see that the obtained titration curves describe the real titration curve well. The following fifth order polynomial is one of the identified inverse models of the titration curve:

Table 2. Experimental Data for the pH Neutralization Process

$c_{f,a}$ = 0.01 mol/L
$c_{c,b}$ = 0.1 mol/L
Reactor volume (V) = 2.67 L
Sampling time = 1 sec
Flow rate of influent stream (F) = 0.4 L/min
Flow rate of titrating stream (u) = 0 − 0.15 L/min
Step and pulse inputs:
Initial flow rate of titrating stream = 0.020 L/min
Magnitudes of step inputs = 0.030 L/min and 0.034 L/min
Magnitude of pulse input = 0.034 L/min
Width of pulse input = 2 min

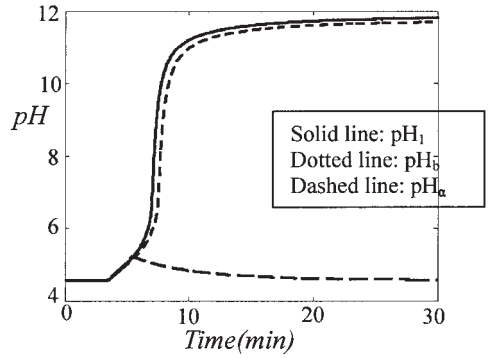

Figure 12. Responses of the experimental pH neutralization process.

$$\frac{c_b(t)}{c_{c,b}} = -2.6811 + 1.7774\,\mathrm{pH}(t) - 0.45529\,\mathrm{pH}^2(t) + 5.7795 \times 10^{-2}\,\mathrm{pH}^3(t) - 3.6333 \times 10^{-3}\,\mathrm{pH}^4(t) + 9.0516 \times 10^{-5}\,\mathrm{pH}^5(t) \quad (28)$$

Figure 14 shows the control performances of the linearizing PI controller. For the linear PI controller, $K_c = 1.414\omega V - F$ and $\tau_1 = (K_c/\omega^2 V)$, where $\omega = 0.25$ is used.[22] Eq. 28 is used as the inverse of the nonlinear static function. Excellent control performances of the linearizing controller for the set point changes are obtained regardless of set point levels.

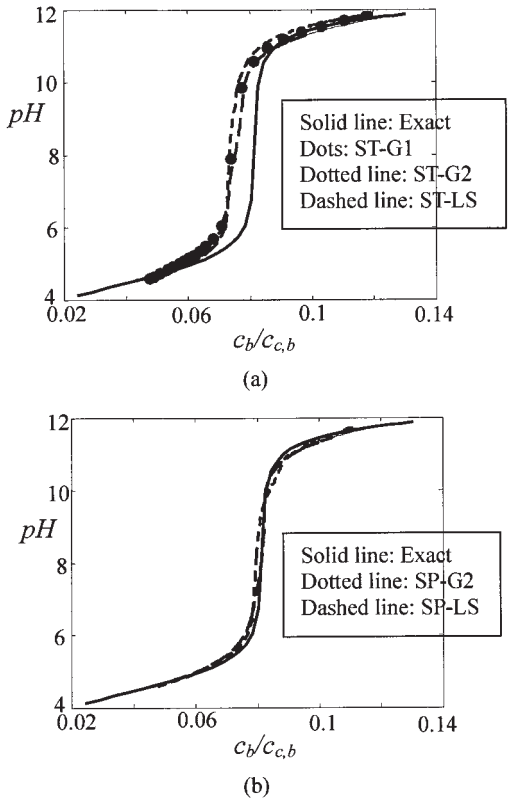

Figure 13. Estimated titration curves of the experimental pH neutralization process.

(a) Step response methods and (b) step and pulse response methods.

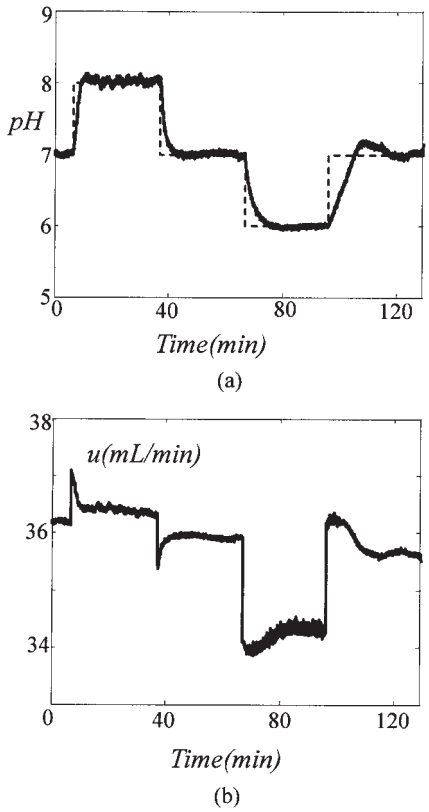

Figure 14. Control results for the experimental pH neutralization process.

(a) pH trajectory (solid line) and set-point (dotted line), and (b) flow rate of the titrating stream.

Conclusions

Simple identification methods to estimate the nonlinear static function of the Wiener-type nonlinear process have been proposed in this research. To activate the process, two step inputs with different sizes, step, and pulse inputs, or two square wave inputs are used and the nonlinear static function is estimated independently regardless of the identification of the linear dynamic subsystem. From two step responses with different magnitudes, discrete points of the nonlinear static function are obtained in a simple graphical method, and a continuous function is obtained with convergent iterations. A parametric model of the nonlinear static function is obtained with the least squares method. Instead of two step responses, we can use step and pulse responses and two square wave responses given via the relay feedback technique. The identified nonlinear static function can be used to linearize the Wiener-type nonlinear process.

In field, PI/PID control systems are designed still from first order plus time delay models identified by graphical and simple least squares methods.[18] The proposed methods share the simplicities of such simple methods for linear processes and can be used as basic identification methods before other elaborate methods are tried to identify nonlinear processes in detail.

Acknowledgments

This work was supported by the Korea Research Foundation Grant funded by the Korean Government (MOEHRD) (R05–2003-000–11208–0).

Literature Cited

1. Haber R, Unbehauen H. Structure identification of nonlinear dynamic systems—a survey on input/output approaches. *Automatica*. 1990;26:651-677.
2. Zhu Y. Estimation of an N-L-N Hammerstein-Wiener model. *Automatica*. 2002;38:1607-1614.
3. Kalafatis A, Arifin N, Wang L, Cluett WR. A new approach to the identification of pH process based on the Wiener model. *Chem Eng Sci*. 1995;50:3693-3701.
4. Vörös J. Parameter identification of Wiener systems with discontinuous nonlinearities. *Systems & Control Letters*. 2001;44:363-372.
5. Pottmann M, Unbehauen H, Seborg DE. Application of a general multi-model approach for identification of highly nonlinear processes—a case study. *Int J Control*. 1993;57:97-120.
6. Bai E. An optimal two-step identification algorithm for Hammerstein-Wiener nonlinear systems. *Automatica*. 1998;34:333-338.
7. Sung SW. System identification method for Hammerstein processes. *Ind Eng Chem Res*. 2002;41:4295-4302.
8. Balestrino A, Landi A, Ould-Zmirli M, Sani L. Automatic nonlinear auto-tuning method for Hammerstein modeling of electrical drives. *IEEE Trans Ind Electron*. 2001;48:645-655.
9. Park HC, Koo DG, Youn JH, Lee J, Sung SW. Relay feedback approaches for the identification of Hammerstein-type nonlinear processes. *Ind Eng Chem Res*. 2004;43:735-740.
10. Luyben WL, Eskinat E. Nonlinear auto-tune identification. *Int J Control*. 1994;59:595-626.
11. Henson MA, Seborg DE. *Nonlinear Process Control*. New Jersey: Prentice-Hall; 1997.
12. Huang H, Lee M, Tang Y. Identification of Wiener model using relay feedback test. *J Chem Eng of Japan*. 1998;31:604-612.
13. Huang HP, Lee MW, Tsai CY. Structure Identification for Nonlinear Models. Proceedings of 6th IFAC Symposium on Dynamics and Control of Process Systems, Jejudo Island, Korea, 2001:748-753.
14. Sung SW, Lee J. Modeling and control of Wiener-type processes. *Chem Eng Sci*. 2004;59:1515-1521.
15. Bai E. Frequency domain identification of Wiener models. *Automatica*. 2003;39:1521-1530.
16. Ljung L. *System Identification—Theory for the User*. 2nd ed. New Jersey: Prentice-Hall; 1999.
17. Mills PM, Zomaya AY, Tade MO. *Neuro-Adaptive Process Control: A Practical Approach*. New York: Wiley; 1993.
18. Åström KJ, Hägglund T. *PID Controllers*. 2nd ed. Research Triangle Park, NC: ISA; 1998.
19. Seborg DE, Edgar TF, Mellichamp DA. *Process Dynamics and Control*. 2nd ed. New York: Wiley; 2004.
20. Park HC. Simple Approaches for the Identification of Wiener and Hammerstein-Wiener Nonlinear Processes. PhD Thesis, Kyungpook National University, Daegu, Korea, 2004.
21. Wright RA, Kravaris C. Nonlinear control of pH process using the strong acid equivalent. *Ind Eng Chem Res*. 1991;30:1561-1572.
22. Lee J, Lee SD, Kwon YS, Park S. Relay feedback method for tuning of nonlinear pH control system. *AIChE J*. 1993;30:1093-1096.

Appendix: Convergence Proof of ST-G2

The ST-G2 method can be considered as finding $v_1(t)$ iteratively. Mathematical induction is used to prove the convergence.

Assume that

$$v_1^k(t) = f(\alpha^{k+1} v_1(t))/\alpha^{k+1}$$

Then Eq. 6 becomes

$$v_1^k(t) = f(\alpha^{k+1} v_1(t))/\alpha^{k+1} = f(\alpha^{k+1} f^{-1}(y_1(t)))/\alpha^{k+1} = f_{k+1}^{-1}(y_1(t))$$

Because $f_{k+1}^{-1}(y_1(t)) = f(\alpha^{k+1} f^{-1}(y_1(t)))/\alpha^{k+1}$, we have

$$v_1^{k+1}(t) = f_{k+1}^{-1}(y_\alpha(t))/\alpha = f(\alpha^{k+1} f^{-1}(y_\alpha(t)))/\alpha^{k+2} = f(\alpha^{k+1} v_\alpha(t))/\alpha^{k+2} = f(\alpha^{k+2} v_1(t))/\alpha^{k+2}$$

Hence, $v_1^k(t) = f(\alpha^{k+1} v_1(t))/\alpha^{k+1}$ is valid for any k, because $v_1^0(t) = y_\alpha(t)/\alpha = f(v_\alpha(t))/\alpha = f(\alpha v_1(t))/\alpha$.

The ST-G2 method converges to

$$\lim_{k\to\infty} v_1^k(t) = \lim_{k\to\infty} \frac{f(\alpha^{k+1} v_1(t))}{\alpha^{k+1}} = \lim_{k\to\infty} f'(\alpha^{k+1} v_1(t)) v_1(t) = f'(0) v_1(t)$$

for $0 < \alpha < 1$ and a finite $f'(0)$.

Manuscript received Aug. 21, 2004, and revision received Aug. 15, 2005.